

Supplementary Materials for
Down-regulation of Phosphoserine Phosphatase Potentiates Tumor Immune
Environments to Enhance Immune Checkpoint Blockade Therapy

Zhi-Peng Peng[#], Xing-Chen Liu[#], Yong-Hao Ruan, Da Jiang, Ai-Qi Huang, Wan-Ru

Ning, Ze-Zhou Jiang, Limin Zheng^{*}, Yan Wu^{*}

[#] These authors contributed equally

^{*}Corresponding author

Email: wuyan32@mail.sysu.edu.cn (Y.W.)

zhenglm@mail.sysu.edu.cn (L.Z.)

Supplementary materials include:

Supplementary Materials and Methods

Supplementary Figures: Fig. S1 to S12

Supplementary Tables: Table S1 to S5

Supplementary Materials and Methods

Cell lines

Hepa1-6 mouse hepatocellular carcinoma cells, PLC/PRF/5 human hepatocellular carcinoma cells, SNU449 human hepatocellular carcinoma cells, and HEK 293T cells were purchased from American Type Culture Collection (ATCC). Their identities were verified by the STR method. Hepa1-6 and HEK 293T were grown in DMEM (C11995500BT, Gibco), PLC/PRF/5 and SNU449 were grown in RPMI 1640 (C11875500BT, Gibco), with 10% fetal bovine serum (FBS, 10099-141, Gibco), 100 units/ml penicillin (AP231, GENVIEW) and 100 µg/ml streptomycin antibiotics (AS325, GENVIEW). All cell lines were regularly tested for mycoplasma contamination using the single-step polymerase chain reaction (PCR) method.

Plasmids, shRNA and lentivirus production

pLKO.1 plasmid was obtained from Addgene (10878). Lentiviral shRNAs (Supplementary Table S3) were purchased from Sangon Biotech (Shanghai, China). For lentivirus productions, the lentivirus expression vector containing the target sequence was co-transfected into HEK 293T cells with packaging plasmid psPAX2 (Addgene, 12260) and envelope plasmid pMD2.G (Addgene, 12259) by Polyethylenimine Linear (PEI, 24765, Polysciences). The lentivirus supernatant was harvested and stored in aliquots at -80°C until use. The stable PSPH knockdown cell lines were established by infecting PLC/PRF/5 and SNU449 cells with lentivirus expressing the target sequence and selected by puromycin treatment.

In vitro culture of PLC/PRF/5, SNU449 and Hepa1-6

In some experiments, PLC/PRF/5 and SNU449 were left untreated or treated with human recombinant TNF- α (5 ng/ml, 210-TA-010, R&D Systems), human recombinant IL-1 β (5 ng/ml, 201-LB-005, R&D Systems), or human recombinant IFN- γ (5 ng/ml, 285-IF-100, R&D Systems) for 24 hours. In some experiments, PLC/PRF/5 and SNU449 were stimulated with human recombinant TNF- α in the presence or absence of S-(5'-Adenosyl)-L-methionine (SAM, 2 mM, A7007, Sigma-Aldrich), N-Acetyl-L-cysteine (NAC, 1mM for SNU449; 5mM for PLC/PRF/5, A7250, Sigma-Aldrich), 3-Deazaadenosine hydrochloride (3-DZA, 5 μ M, HY-W013332A, MCE), AG490 (10 μ M, HY-12000, MCE), or DMSO for 24 hours. In some other experiments, Hepa1-6 was treated with Metformin (60mM, HY-17471A, MCE) for 12 hours.

UHPLC-MRM-MS/MS analysis of metabolites

Fresh HCC tumor and paired non-tumor liver tissues were cut into small pieces and stored at -80°C before use. UHPLC-MRM-MS/MS was performed by Shanghai Biotree Biotech Limited Company (Shanghai, China), and the abundance of metabolites (D-3-Phosphoserine, Glycine, L-Serine, L-Methionine) was measured and compared to internal standard controls according to protocols.

Isolation of leukocytes from tissues

For isolation of tumor-infiltrating leukocytes from mouse tumors, fresh tumors were cut into small pieces and digested in RPMI 1640 medium supplemented with 0.002% DNase I (DN25, Sigma-Aldrich), 0.05% collagenase IV (C5138, Sigma-Aldrich), 50 μ g/ml hyaluronidase (H1136, Sigma-Aldrich), 30 μ g/ml Collagenase XI (C7657,

Sigma-Aldrich), 20% FBS, 100U/ml penicillin and 100µg/ml streptomycin at 37°C for 40 minutes. Dissociated cells were separated by Ficoll density-gradient centrifugation. Leukocytes were stained with PE/Cyanine7-conjugated anti-mouse CD11b (101216, Biolegend), BV421-conjugated anti-mouse Ly6C (128032, Biolegend), FITC-conjugated anti-mouse Gr-1 (11-5931-85, eBioscience), and PE-CF594-conjugated anti-mouse Ly6G antibodies (562700, Biolegend). Ly6C⁺ monocytes and F4/80⁺ macrophages were then purified using a MoFlo XDP Cell Sorter (Beckman Coulter, Brea, U.S.). The purified cells were then used for direct analysis, or in vivo cell transfusion experiments.

The Cancer Genome Atlas (TCGA) data analysis

The TCGA clinical data were downloaded from the data portal of Genomic Data Commons. Gene expression profiles of 50 patients with paired tumor and non-tumor data were enrolled for analysis.

Quantitative real-time PCR (Q-PCR)

Total RNA was extracted using TRIzol reagent (AM9738, Life Technologies) and then used to synthesize cDNA with 5X All-In-One RT MasterMix (G486, Abm). Sequences of the primers used for PCR analysis were listed in [Supplementary Table S3](#). Quantitative PCR was performed according to a standard protocol using the SYBR Green Real-Time PCR Mix (QPS-201, TOYOBO) in LightCycler 480 System (Roche, Basel, Switzerland). To determine the relative fold change of different genes, their levels of expression were normalized to those of β-actin.

Western blotting (WB)

Primary antibodies used included: PSPH Rabbit Polyclonal antibody (14513-1-AP, Proteintech), MTHFD1L Rabbit Polyclonal antibody (16113-1-AP, Proteintech), ALDH1L2 Rabbit Polyclonal antibody (21391-1-AP, Proteintech), MAT2A Rabbit Polyclonal antibody (55309-1-AP, Proteintech), ALDH1L1 Rabbit Polyclonal antibody (17390-1-AP, Proteintech), MAT1A Rabbit Polyclonal antibody (12395-1-AP, Proteintech), H3K27me3 Rabbit Monoclonal antibody (9733, Cell Signaling Technology), Histone H3 Rabbit Monoclonal antibody (4499, Cell Signaling Technology), phospho-STAT3^{Tyr705} Rabbit Monoclonal antibody (9145, Cell Signaling Technology, Danvers, U.S.), STAT3 Mouse Monoclonal Antibody (9139, Cell Signaling Technology), β -actin Mouse Monoclonal Antibody (ab8226, Abcam). HRP-linked goat anti-rabbit/mouse IgG antibodies were purchased from Cell Signaling Technology.

Immunohistochemistry (IHC) staining

Paraffin-embedded and formalin-fixed samples were cut into 4 μ m sections. After incubation with primary antibodies against PSPH (14513-1-AP, Proteintech), sections were stained with corresponding secondary antibodies and visualized with diaminobenzidine and 3-amino-9-ethylcarbazole in an Envision System. The intensity of protein expression was quantified using ImagePro Plus software (Media Cybernetics, Maryland, U.S.).

Multiplex immunofluorescence (IF) staining

For multiplex immunofluorescence analysis of patient samples, Paraffin-embedded and formalin-fixed samples were cut into 4 μ m sections. The sections were incubated

with primary antibodies against PSPH (14513-1-AP, Proteintech), F4/80 (70076, Cell Signaling Technology), CD8a (98941, Cell Signaling Technology), Ly6C (ab15627, Abcam), or PSPH (14513-1-AP, Proteintech), CD68 (M087629, Dako), CD8a (85336, Cell Signaling Technology), H3K27me3 (9733, Cell Signaling Technology), phospho-STAT3^{Tyr705} (9145, Cell Signaling Technology). Immunofluorescence signals were amplified by a tyramide signal amplification kit (PPK007100100, Panovue) for visualization. Nuclei were counterstained with DAPI (10236276001, Roche).

Immunofluorescence staining images were visualized by the ZEISS microscope (LSM780, Germany). The intensity of protein expression was evaluated using Zeiss ZEN software (LSM780, Germany), and positive cells were quantified using ImagePro Plus software (Media Cybernetics, Maryland, U.S.). Results were expressed as mean \pm SEM in high-powered fields.

Flow cytometry

Cell surface markers were determined by direct staining with anti-mouse CD45-BV570 (103135, Biolegend), anti-mouse Ly-6G-PE-cf594 (562700, BD Biosciences), anti-mouse Ly-6C-BV421 (128032, Biolegend), anti-mouse CD11b-AF700 (101222, Biolegend), anti-mouse F4/80-APC (123116, Biolegend), anti-mouse CD3-FITC (100203, Biolegend), anti-mouse CD8a-PE (100708, Biolegend). In some experiments, to measure intracellular perforin or granzyme B production, lymphocytes were cultured at 37°C for 12 hours, stained with surface markers, fixed, permeabilized with IntraPre Reagent (A07803, Beckman), and further stained with anti-mouse Perforin-APC (154404, Biolegend) and anti-mouse

Granzyme B-PC7 (372214, Biolegend). Hepa1-6 apoptosis was quantified using an annexin V apoptosis detection kit (K201, Biovision) following the manufacturer's instructions. Data were acquired with CytoFLEXS flow cytometer (Beckman Coulter, Brea, U.S.) and evaluated with FlowJo software version V10 (Tree Star, Ashland, U.S.) (Supplementary Fig. S12).

Intracellular ROS detection

PLC/PRF/5 and SNU449 cells were stimulated with human recombinant TNF- α for 24 hours, and then incubated with dichlorofluorescein diacetate (5 μ M, 2044-85-1, Sigma-Aldrich) for 30 minutes at 37°C. Cells were analyzed by CytoFLEXS flow cytometer (Beckman Coulter, Brea, U.S.).

Cell viability assay

shPLKO-Hepa1-6 and shPSPH-Hepa1-6 cells were seeded into 96-well plates (3000 cells per well) for 24 hours. In some experiments, Hepa1-6 was seeded into 96-well plates and treated with Metformin for 12 hours. 10 μ l CCK-8 (ab228554, Abcam) was added into 190 μ l medium to each well for incubation at 37°C for 2 hours, then the optical density (OD) was measured by varioskans lux (Thermo Scientific, Waltham, U.S.) at 450 nm.

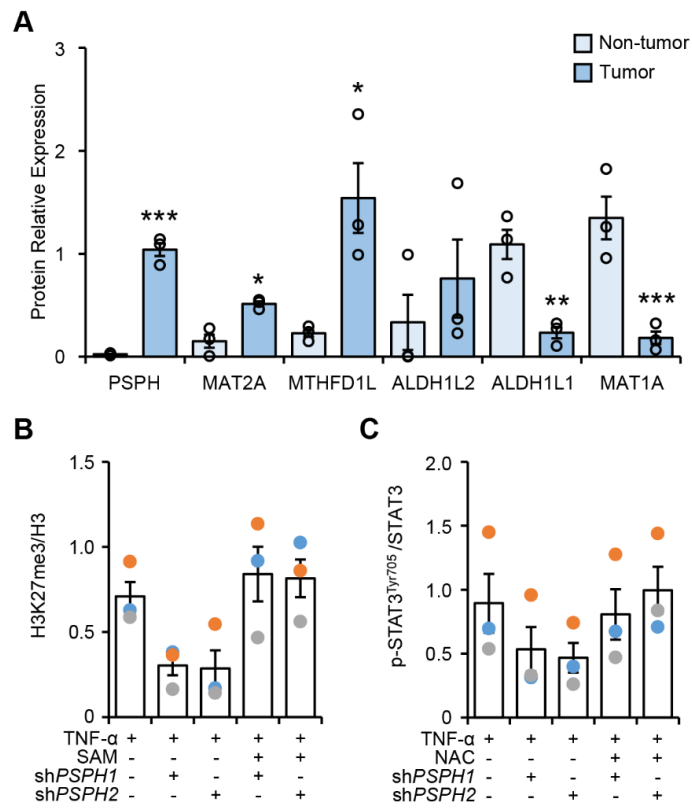
Enzyme-linked immunosorbent assay (ELISA)

Concentrations of CCL2, CXCL10 (88-7399-88 / CHC2363, Invitrogen), SAM, SAH (SAM, MM-13267H1, MEIMIAN; SAH, MM-13268H1, MEIMIAN), GSH, and GSSG (GSH/GSSG, S0053, Beyotime) were determined by ELISA kits according to the manufacturer's instructions.

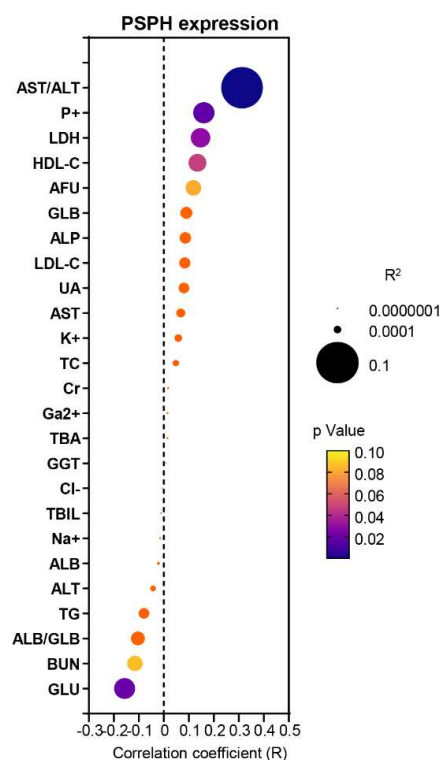
RNAseq and enrichment analysis

PLC/PRF/5 and SNU449 were stimulated with human recombinant TNF- α for 24 hours. RNA of the cells was extracted by TRIzol method, and RNA-sequencing was processed on an Illumina HiSeq 2500 platform (Illumina, San Diego, U.S.). The gene matrix files were generated with RNA express app (Illumina) and analyzed using T-test comparison and log₂ ratio of classes. GO term Enrichment was performed using DAVID (david.ncifcrf.gov) and Gene Set Enrichment Analysis (GSEA) was performed using the GSEA v3.0 software (<http://www.broadinstitute.org/gsea/index.jsp>) with 1000 gene-set permutations, using the gene-ranking metric T-test with the signatures (WP_JAK_STAT_SIGNALING_PATHWAY; WP_MAPK_SIGNALING_PATHWAY; WP_PI3KAKT_SIGNALING_PATHWAY; WP_TNF_ALPHA_SIGNALING_PATHWAY).

For further details regarding the antibodies and reagents used in this study, please refer to [Supplementary Table S4](#) and [Supplementary Table S5](#).



Supplementary Fig. S1 The densitometry data for Fig. 1D, 3C, and 3H.



Supplementary Fig. S2 Correlation between tumor PSPH levels and peripheral

markers in patients with HCC. Correlation between the levels of PSPH in tumor

tissues and indicated markers in peripheral blood were monitored. n = 221. Statistical

methods: Pearson correlation and linear regression analysis. AST: aspartate

aminotransferase; ALT: alanine aminotransferase; LDH: lactate dehydrogenase;

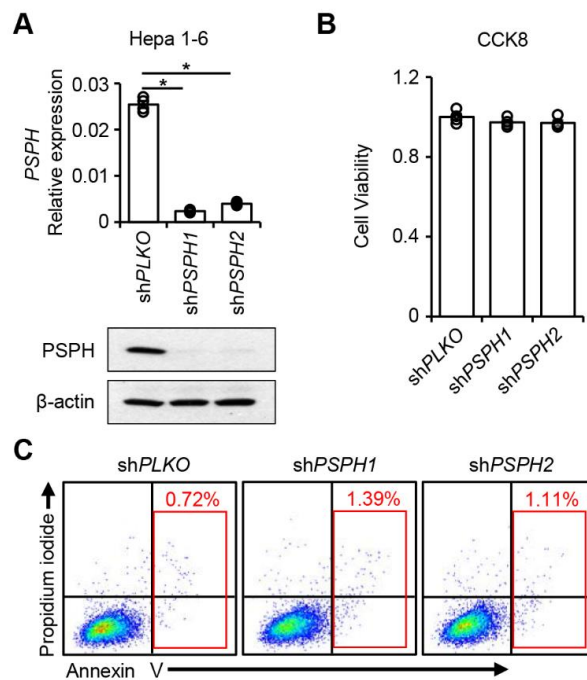
HDL-C: high-density lipoprotein cholesterol; AFU: alpha-L-fucosidase; GLB:

globulin; ALP: alkaline phosphatase; LDL-C: low-density lipoprotein cholesterol;

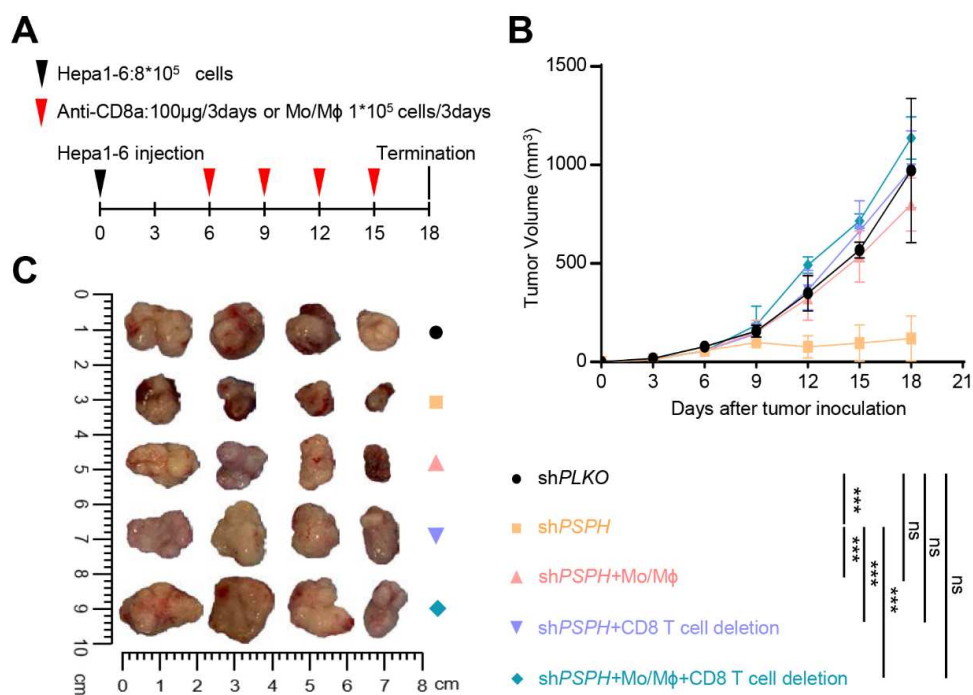
UA: uric acid; TC: total cholesterol; Cr: creatinine; TBA: total bile acid; GGT:

gamma-glutamyl transpeptidase; TBIL: total bilirubin; ALB: albumin; TG:

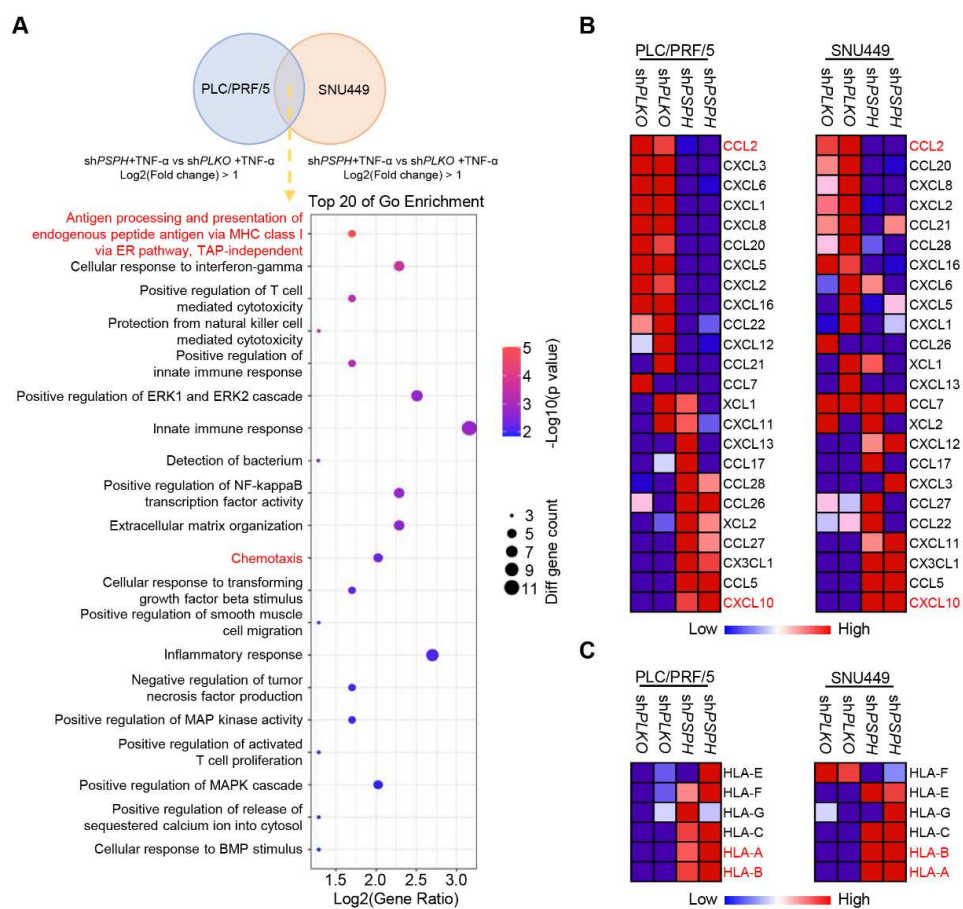
triglyceride; BUN: blood urea nitrogen; GLU: glucose.



Supplementary Fig. S3 shPSPH transfection does not affect tumor cell viability and apoptosis *in vitro*. A-C, Hepa1-6 cells were transfected with shPSPH1, shPSPH2, or shPLKO control. **A**, Efficiency of shPSPH1 and shPSPH2 transfection was determined by Q-PCR and western blotting. **B**, Cell viability was measured by the CCK8 analyzing kit. **C**, Cell apoptosis was analyzed by flow cytometry. n = 4. Data are mean \pm SEM. Statistical methods: Welch's t-test (**A**), Student's t test (**B**). *p < 0.05.

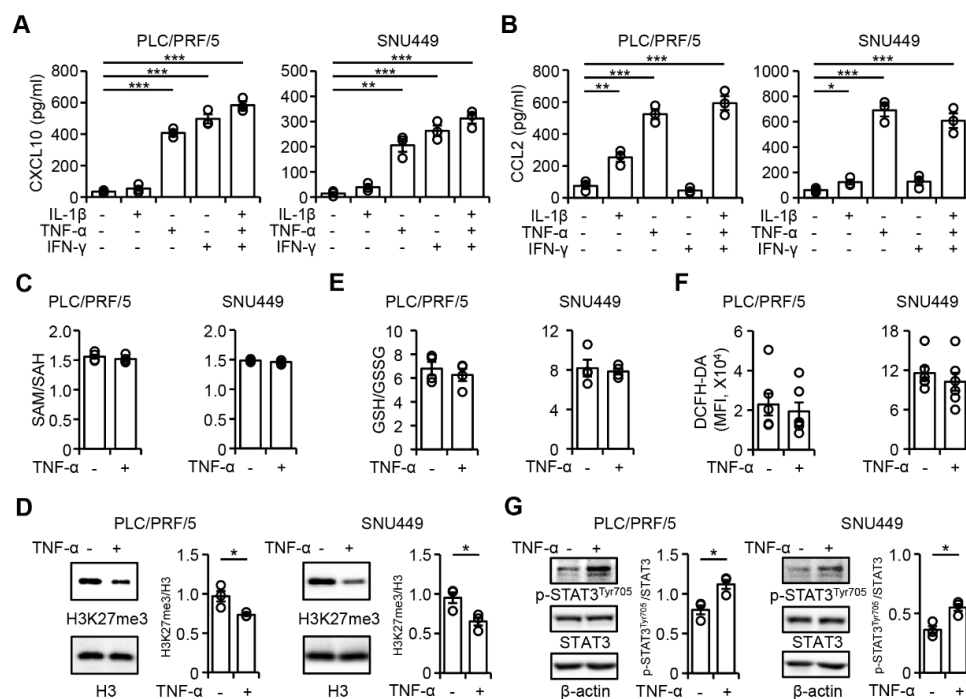


Supplementary Fig. S4 The in vivo anti-tumor effects of shPSPH depended on the reduced macrophages and increased CD8⁺ T cells infiltration. A-C, C57BL/6 Mice bearing Hepa1-6 tumors were intraperitoneally injected with anti-mouse CD8a antibodies or intratumorally injected with mice Ly6C⁺ monocytes and F4/80⁺ macrophages at indicated times (A). Tumor growth (B, C (day 18)) was monitored. n = 4. Statistical methods: Two-way ANOVA with Bonferroni's multiple comparisons test (B). *p < 0.001; ns, no significance.**

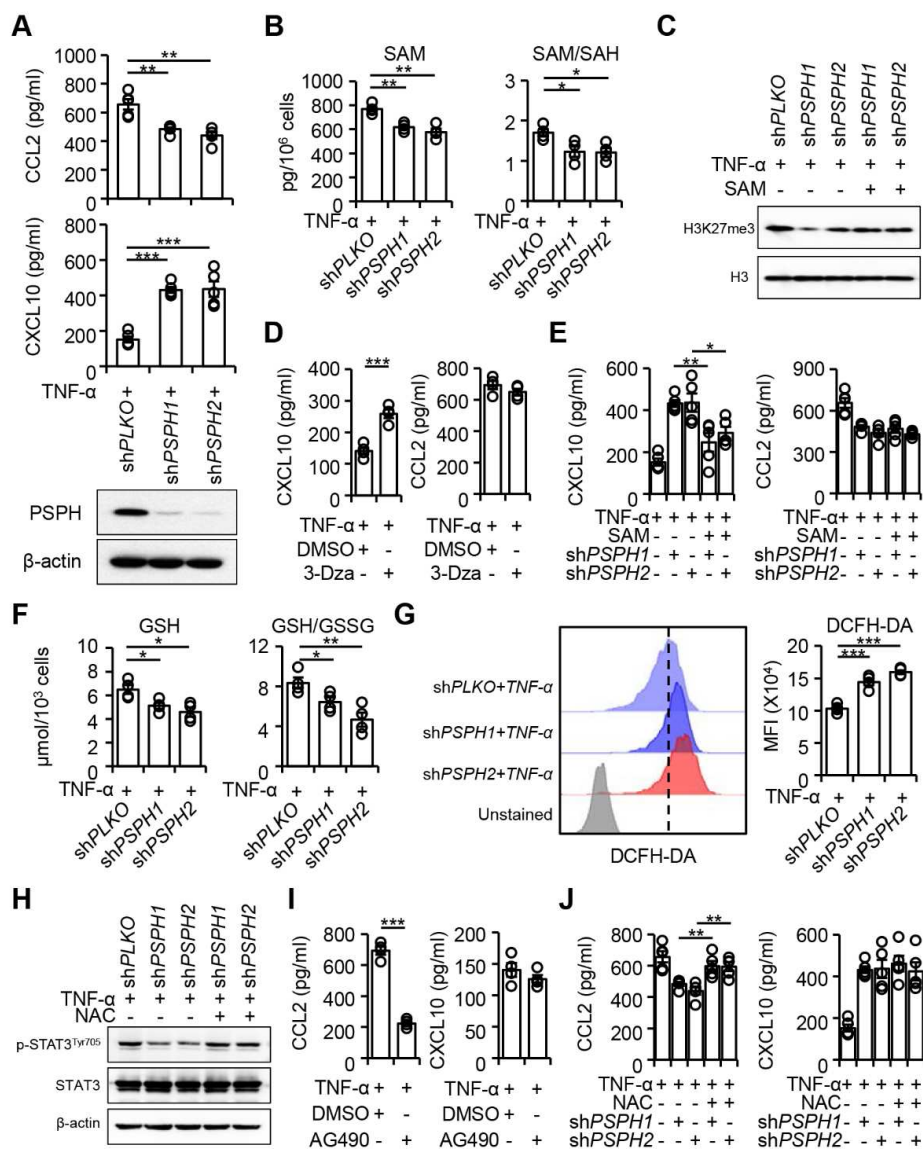


Supplementary Fig. S5 Genes differentially expressed by shPSPH- and shPLKO-transfected hepatoma cells. A-C, RNA-sequencing was performed to identify differentially expressed genes between the shPSPH and shPLKO transfected hepatoma cells (PLC/PRF/5 or SNU449 cells). The overlap genes between PLC/PRF/5 and SNU449 were subjected to the GO term enrichment analysis. n = 2 (A). Differentially expressed chemokines and MHC molecules were analyzed (B-C).

Supplementary Fig. S6



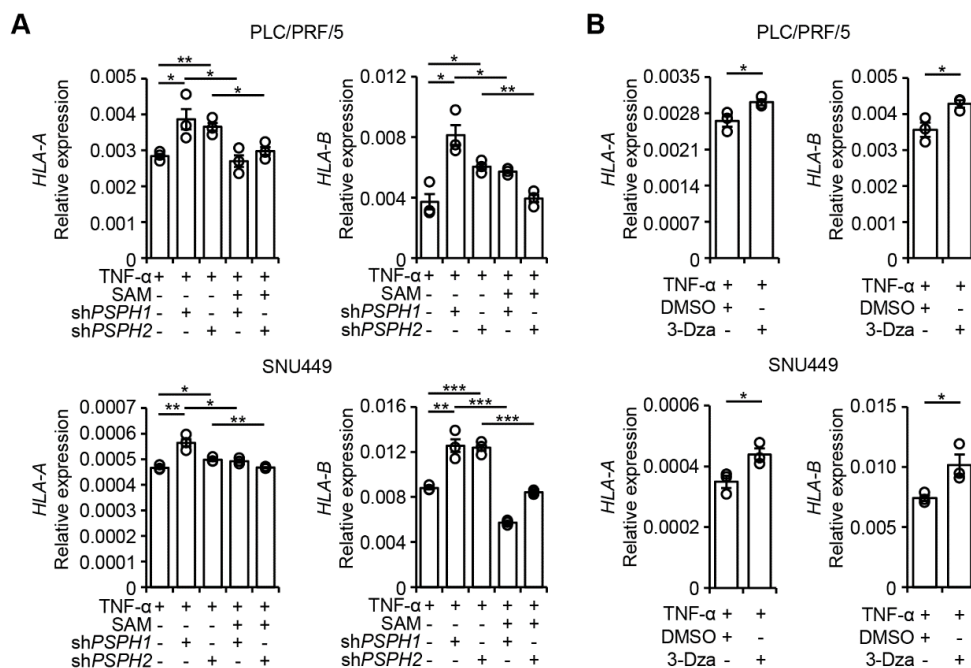
Supplementary Fig. S6 Effects of cytokines on CCL2, CXCL10, SAM/SAH, H3K27me3, GSH/GSSG, ROS, and p-STAT3^{Tyr705} expression by hepatoma cells *in vitro*. A-B, PLC/PRF/5 and SNU449 cells were treated with the indicated combination of cytokines. Their production of CXCL10 (A) and CCL2 (B) were measured through ELISA. n = 3. C-G, PLC/PRF/5 and SNU449 cells were treated with TNF- α . Levels of SAM/SAH (C), H3K27me3 (D), GSH/GSSG (E), ROS (F), and p-STAT3^{Tyr705} (G) in these cells were analyzed through ELISA, Western blotting, or Flow cytometry. (C, E, n = 4, D, G, n = 3, F, n = 6). Data are mean \pm SEM. Statistical methods: Student's t test. *p < 0.05, **p < 0.01, ***p < 0.001.



Supplementary Fig. S7 PSPH regulates tumor release of CXCL10 and CCL2

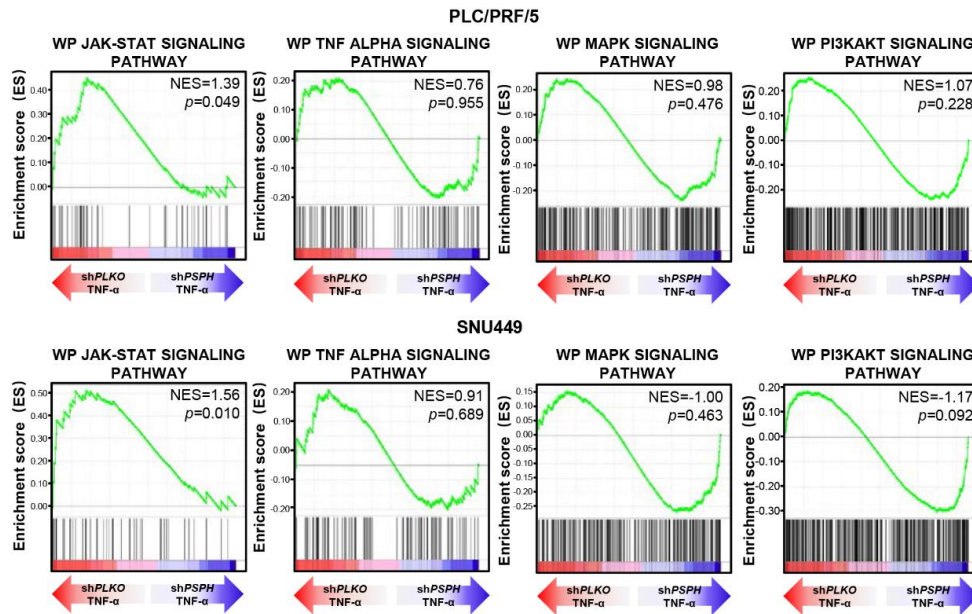
through the SAM and GSH pathways respectively. SNU449 cells were left untreated or transfected with shPLKO or shPSPH, and treated with TNF- α . **A**, Western blotting showed PSPH, and ELISA showed CCL2, CXCL10 levels in shPLKO or shPSPH tumor cells (n = 5). **B**, SAM and SAM/SAH were measured in shPLKO or shPSPH tumor cells (n = 4). **C**, Western blotting showed H3K27me3 in

shPLKO or shPSPH tumor cells, in the presence or absence of supplemented SAM (n = 3). **D-E**, ELISA showed CCL2 and CXCL10 levels in 3-Dza -treated or -untreated tumor cells (n=4, **D**), or in shPLKO or shPSPH transfected tumor cells, in the presence or absence of supplemented SAM (n=5, **E**). **F**, GSH and GSH/GSSG were measured in shPLKO or shPSPH tumor cells (n = 4). **G**, Flow cytometry analysis showed ROS levels in shPLKO or shPSPH tumor cells (n = 4). **H**, Western blotting showed STAT3, p-STAT3^{Tyr705} in shPLKO or shPSPH tumor cells, in the presence or absence of supplemented NAC (n = 3). **I-J**, ELISA showed CCL2 and CXCL10 levels in AG490 -treated or -untreated tumor cells (n = 4, **I**), or in shPLKO or shPSPH transfected tumor cells, in the presence or absence of supplemented NAC (n = 5, **J**). Data are mean ± SEM. Statistical methods: Student's t test (**A, B, D, E, F, G, I, J**). *p < 0.05, **p < 0.01, ***p < 0.001.

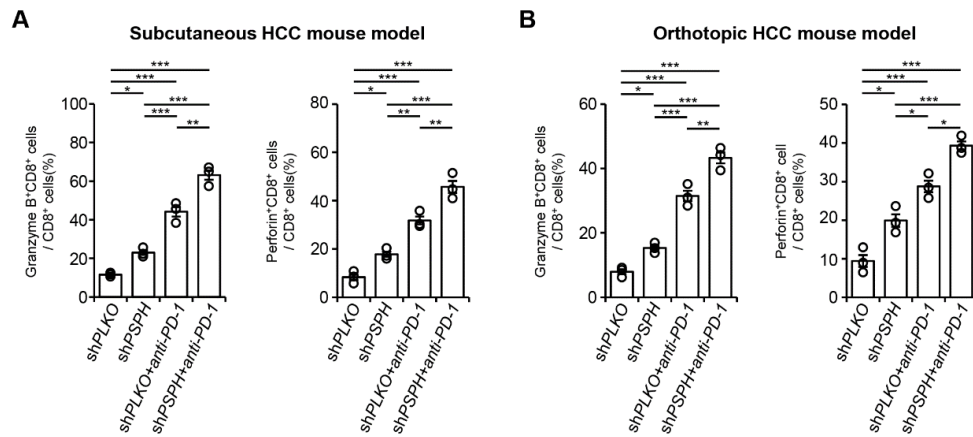


Supplementary Fig. S8 PSPH regulates tumor expression of *HLA-A* and *HLA-B*

through the SAM pathway. A-B, Q-PCR analysis showed the levels of *HLA-A* and *HLA-B* expression on TNF- α -treated PLC/PRF/5 or SNU449 cells, which were transfected with shPLKO or shPSPH, in the presence or absence of supplemented SAM (A), or on TNF- α -treated PLC/PRF/5 or SNU449 cells, in the presence of DMSO or 3-Dza (B). n = 3. Data are mean \pm SEM. Statistical methods: Student's t test (A, B). *P < 0.05, **P < 0.01, ***P < 0.001.

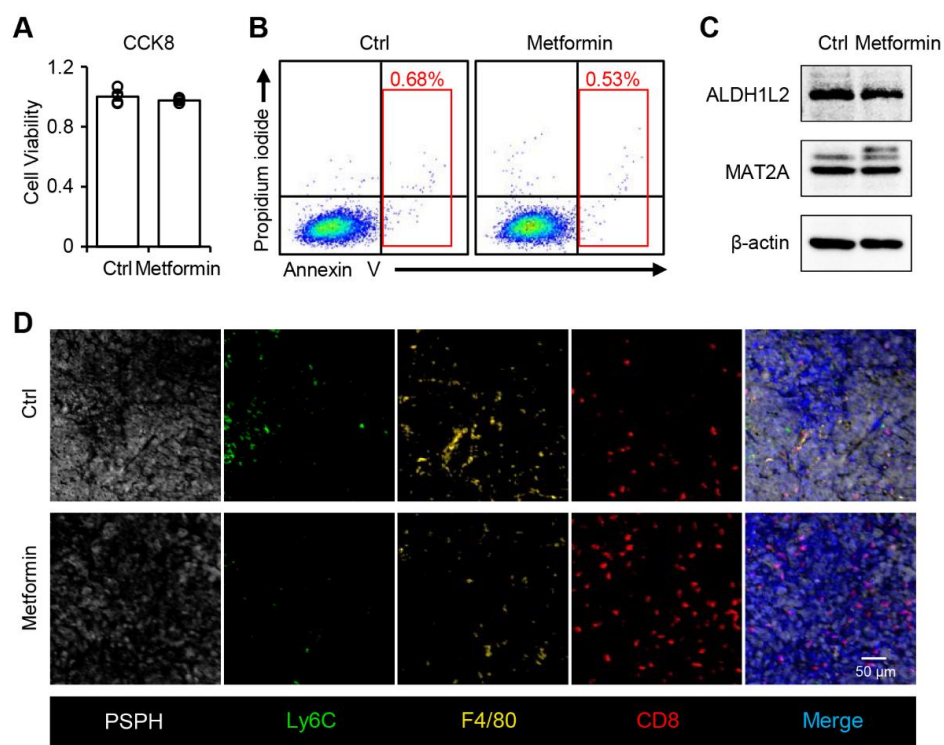


Supplementary Fig. S9 Enrichment of different signaling pathways in *shPSPH*- vs *shPLKO*- transfected hepatoma cells. GSEA analysis showed the enrichment of indicated signaling pathways in *shPSPH*- vs *shPLKO* transfected PLC/PRF/5 or SNU449 cells. n = 2.

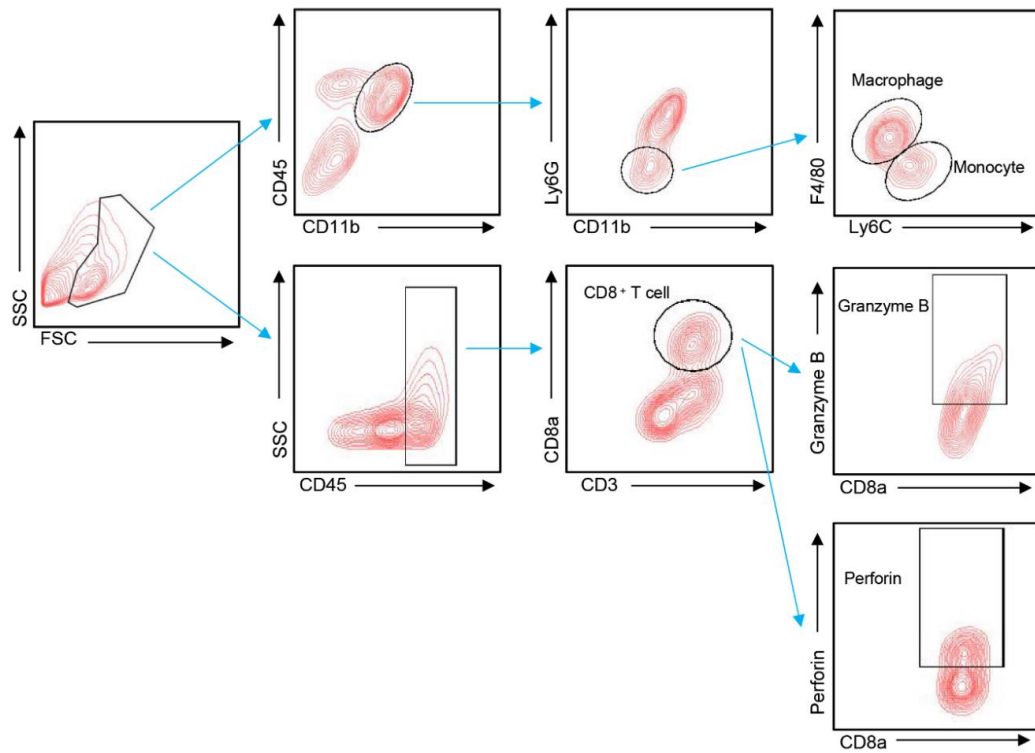


Supplementary Fig. S10 CD8⁺ T cell activities are enhanced in shPSPH-transfected Hepa1-6 tumors *in vivo*. C57BL/6 mice with established shPLKO or shPSPH-transfected Hepa1-6 tumors (subcutaneous (A) or orthotopic (B)) were intraperitoneally injected with or without anti-PD-1 antibodies. Flow cytometry showed the expression of Granzyme B and perforin in tumor-infiltrating CD8⁺ T cells on Day 21. n = 3. Data are mean ± SEM. Statistical methods: Student's t test (A, B).

*p < 0.05, **p < 0.01, ***p < 0.001; ns, no significance.



Supplementary Fig. S11 Metformin mimics the effects of shPSPH in regulating tumor immune compositions. **A-B**, Hepa1-6 cells were treated with or without metformin for 12 hours. **A**, Cell viability was measured by CCK8 analyzing kit. **B**, Cell apoptosis was analyzed by flow cytometry. $n = 4$. **C**, Effects of Metformin on ALDH1L2 and MAT2A expression were determined by western blotting. $n = 4$. **D**, Effects of Metformin on the expression of PSPH, and the infiltrations of Ly6C⁺ monocytes, F4/80⁺ macrophages, and CD8⁺ T cells in Hepa1-6 tumors in C57BL/6 mice were determined by immunofluorescent analysis. $n = 3$. Data are mean \pm SEM. Statistical methods: Student's t test (**A**).



Supplementary Fig. S12 Flow cytometry gating strategy. For all the flow cytometry data in the figures, we selected CD45-BV570/CD11b-AF700/F4/80-APC triple-positive cells as macrophages and CD45-BV570/CD11b-AF700/Ly6C-BV421 triple-positive cells as monocytes. We selected CD45-BV570/CD3-FITC/CD8a-PE triple-positive cells as CD8⁺ T cells, which were subjected to GranzymeB-PC7 and Perforin-APC analysis.

Supplementary Table S1. Clinical characteristics of HCC patients

Patients characteristics	Cohort 1	Cohort 2
No. of patients	321	30
Age, years (median, range)	49.8, 13-78	49.2, 29-69
Gender (male/female)	286/35	26/4
HBsAg (negative/positive)	32/289	5/25
ALT, U/L (median, range)	49.0, 9-713	87.0, 13-458
AFP, ng/mL (≤ 25 / > 25)	121/200	5/25
Tumor size, cm (≤ 5 / > 5)	153/168	11/19
Tumor multiplicity (solitary/multiple)	239/82	22/8
TNM stage (I/II+III)	212/109	10/20
Tumor differentiation (I+II/III+IV)	193/128	16/14
Cirrhosis (absent/present)	114/207	13/17
Fibrous capsule (absent/present)	226/95	17/13
Intrahepatic metastasis (no/yes)	205/116	20/10
Vascular invasion (absent/present)	250/71	14/16

Abbreviations: HBsAg, hepatitis B surface antigen; ALT, alanine aminotransferase; AFP, α -fetoprotein; TNM, tumor-node-metastasis.

Note: Samples from patients in Cohort 1 were used in Fig. 1J, Fig. S1, Table 1; Samples from patients in Cohort 2 were used in Fig. 1B-I, Fig. 4.

Supplementary Table S2. Univariate and multivariate analysis of factors associated with overall survival of patients with HCC.

Clinical variables	OS						
	Univariate				Multivariate		
				p value	HR	95% CI	p value
Age, years	>50	vs.	≤50	0.595			
Gender	female	vs.	male	0.314			
HBsAg	positive	vs.	negative	0.735			
ALT, U/L	>40	vs.	≤40	0.163			
AFP, ng/ml	>25	vs.	≤25	0.014	1.217	0.815-1.817	0.338
Tumor size, cm	>5	vs.	≤5	<0.001	1.454	0.985-2.145	0.060
Tumor multiplicity	multiple	vs.	solitary	<0.001	0.642	0.389-1.059	0.083
TNM stage	II+III	vs.	I	<0.001	2.872	1.720-4.794	<0.001
Tumor differentiation	III+IV	vs.	I+II	0.077			
Cirrhosis	present	vs.	absent	0.370			
Fibrous capsule	present	vs.	absent	0.796			
Intrahepatic metastasis	yes	vs.	no	0.009	1.212	0.859-1.708	0.273
Vascular invasion	yes	vs.	no	<0.001	1.834	1.238-2.719	0.003
PSPH expression	high	vs.	low	0.001	1.475	1.045-2.082	0.027

HBsAg, hepatitis B surface antigen; ALT, alanine aminotransferase; AFP, a-fetoprotein; TNM, tumor-node-metastasis; PSPH, Phosphoserine Phosphatase; HCC, hepatocellular carcinoma.

Cumulative survival time was estimated by Kaplan-Meier method, and the log-rank test was applied to compare the groups. Cox proportional hazards regression model was used to conduct a multivariate analysis of survival. p values in bold denote statistical significance.

Supplementary Table S3. Sequences for RT-PCR and shRNAs

Primers for RT-PCR		
Genes		Sequences
Human <i>PHGDH</i>	Forward	GGAGGAGGAGGAGGAGATGA
	Reverse	GGCCGCTGTGAGTAGAAGTA
Human <i>PSAT1</i>	Forward	GGGAATTGCTAGCTGTTCCAG
	Reverse	TCAGCACACCTTCCTGCTTT
Human <i>PSPH</i>	Forward	ATCTCCTGACCTTGTGATCCG
	Reverse	GCTGCCGAATCCGTATTTCTAA
Human <i>SHMT2</i>	Forward	GAGCAGAGGTGGTGGATGAA
	Reverse	ATGTAGCCGTGGGTGAGATG
Human <i>MTHFD2</i>	Forward	TGGCTGCGACTTCTCTAATGT
	Reverse	CACTTCCTGCTTGATCTGCTG
Human <i>MTHFD1L</i>	Forward	CAACATCAAGTGCCGAGCTT
	Reverse	AAGAGGAACACCAGCCGTTA
Human <i>ALDH1L2</i>	Forward	TAACACATACAACAAGACAGAT
	Reverse	ATATTCATTTAGAGCTTCCTCA
Human <i>MTHFD1</i>	Forward	CCTGGCTCTCACCATTCTC
	Reverse	ATCCTGCTTCCGTCACTACAA
Human <i>ALDH1L1</i>	Forward	GCCTGGCTTCTGGTGTCTTC
	Reverse	GCCACGTCGGTCTTGTTGTA
Human <i>SHMT1</i>	Forward	CCCGAAACCTGGAATATG
	Reverse	ATGGCAGTGTTCAAATGG
Human <i>MTHFR</i>	Forward	CTACCTCACCTGCCAGTATCTT
	Reverse	AAGCCACCACCAAACCAAAC
Human <i>MAT1A</i>	Forward	CGTGAGTGGAGAAGTGTGAGA
	Reverse	CCGATGTGCTTGATGGTGTC
Human <i>MAT2A</i>	Forward	ACAATCTACCACCTACAGCC
	Reverse	CCAACGAGCAGCATAAGC
Human <i>CCL2</i>	Forward	AACCGAGAGGCTGAGACTAAC
	Reverse	GGAATGAAGGTGGCTGCTATG
Human <i>CXCL10</i>	Forward	TTCAAGGAGTACCTCTCTCTAG
	Reverse	CTGGATTGAGACATCTCTTCTC
Human <i>HLA-A</i>	Forward	TTGAGAGCCTACCTGGATGG
	Reverse	TGGTGGGTCATATGTGTCTTG
Human <i>HLA-B</i>	Forward	CTTCAAGAGCCTCTGGCATC
	Reverse	AGGGGTCACAGTGGACACA
Human β -actin	Forward	GGATGCAGAAGGAGATCACT
	Reverse	CGATCCACACGGAGTACTTG

Mouse <i>PSPH</i>	Forward	ACCGTCATCAGAGAAGAAG
	Reverse	CTTATGCCAGGAGTCAGAT
Mouse <i>CCL2</i>	Forward	AGCCAACCTCTCACTGAAG
	Reverse	CTCTCCAGCCTACTCATTG
Mouse <i>CXCL10</i>	Forward	GGCTCGTCAGTTCTAAGTT
	Reverse	TGATGACACAAGTTCTTCCA
Mouse β -actin	Forward	CCAGGTCATCACTATTGGCAAC
	Reverse	TACGGATGTCAACGTCACAC

Lentiviral shRNA

shRNA	Vector		Sequences
Human sh <i>PSPH1</i>	pLKO.1-H- sh <i>PSPH1</i>	Forward	CCGGTGAGGACGCGGTGTCAGAA ATCTCGAGATTTCTGACACCGCGT CCTCATTTTTG
		Reverse	AATTCAAAAATGAGGACGCGGTG TCAGAAATCTCGAGATTTCTGAC ACCGCGTCCTCA
Human sh <i>PSPH2</i>	pLKO.1-H- sh <i>PSPH2</i>	Forward	CCGGGGATAACGCCAAATGGTAT ATCTCGAGATATAACCATTGGCGT TATCCTTTTTG
		Reverse	AATTCAAAAAGGATAACGCCAAA TGGTATATCTCGAGATATAACCATT TGGCGTTATCC
Mouse sh <i>PSPH1</i>	pLKO.1-M- sh <i>PSPH1</i>	Forward	CCGGAGGCTGAAGTTCTACTTTA ATCTCGAGATTAAGTAGAACTT CAGCCTTTTTTG
		Reverse	AATTCAAAAAGGCTGAAGTTCT ACTTTAATCTCGAGATTAAGTA GAACTTCAGCCT
Mouse sh <i>PSPH2</i>	pLKO.1-M- sh <i>PSPH2</i>	Forward	CCGGACGTTGCTGCAAAGCTCAA TACTCGAGTATTGAGCTTTGCAGC AACGTTTTTTG
		Reverse	AATTCAAAAACGTTGCTGCAAAA GCTCAATACTCGAGTATTGAGCTT TGCAGCAACGT

Supplementary Table S4. Antibodies used in studies.

Name	Supplier	Cat no.	Clone no.
Rabbit Anti-Human PSPH	proteintech	14513-1-AP	
Rabbit Anti-Human MTHFD1L	proteintech	16113-1-AP	
Rabbit Anti-Human ALDH1L2	proteintech	21391-1-AP	
Rabbit Anti-Human ALDH1L1	proteintech	17390-1-AP	
Rabbit Anti-Human MAT2A	proteintech	55309-1-AP	
Rabbit Anti-Human MAT1A	proteintech	12395-1-AP	
Rabbit Anti-Human H3K27me3	Cell Signaling Technology	9733	C36B11
Rabbit Anti-Human Histone H3	Cell Signaling Technology	4499	D1H2
Rabbit Anti-Human p-STAT3 ^{Tyr705}	Cell Signaling Technology	9145	D3A7
Mouse Anti-Human STAT3	Cell Signaling Technology	9139	124H6
Mouse Anti-Human β -Actin	Abcam	ab14935	AC-15
Mouse Anti-Human CD68	Dako	M087629	PG-M1
Rabbit Anti-Human CD8a	Cell Signaling Technology	85336	D8Y8A
Rabbit Anti-Mouse CD8a	Cell Signaling Technology	98941	D4W2Z
Rabbit Anti-Mouse F4/80	Cell Signaling Technology	70076	D2S9R
Rat Anti-Mouse Ly6C	Abcam	ab15627	ER-MP20
PE-CF594 Rat Anti-Mouse Ly-6G	BD Biosciences	562700	1A8
Ly-6G/Ly-6C Monoclonal Antibody, FITC	eBioscience	11-5931-85	RB6-8C5
PC7-conjugated anti-mouse CD11b	Biolegend	101216	M1/70
BV 570 anti-mouse CD45 Antibody	Biolegend	103135	30-F11
BV421 anti-mouse Ly-6C Antibody	Biolegend	128032	HK1.4
AF700 anti-mouse CD11b Antibody	Biolegend	101222	M1/70
APC anti-mouse F4/80 Antibody	Biolegend	123116	BM8
PE anti-mouse CD8a Antibody	Biolegend	100708	53-6.7
FITC anti-mouse CD3 Antibody	Biolegend	100203	17A2

APC anti-mouse Perforin Antibody	Biolegend	154404	S16009B
PC7 anti-mouse Granzyme B Antibody	Biolegend	372214	QA16A02
Rat IgG2a isotype control antibody	Bioxcell	BP0089	2A3
Anti-mouse CD8a antibody	Bioxcell	BE0004	53-6.7
Anti-mouse PD-1 antibody	Bioxcell	BE0146	RMP1-14
HRP-conjugated goat anti-rabbit IgG	Cell Signaling Technology	7074	
HRP-conjugated goat anti-mouse IgG	Cell Signaling Technology	7076	

Supplementary Table S5. Reagents used in studies.

Name	Supplier	Cat no.
RPMI 1640 medium	Thermo Fisher Scientific	C11875500BT
DMEM	Thermo Fisher Scientific	C11995500BT
FBS	Gibco	10099-141
Penicillin	GENVIEW	AP231
Streptomycin	GENVIEW	AS325
Hepes	Sigma-Aldrich	H4034
DNase I	Sigma-Aldrich	DN25
Collagenase IV	Sigma-Aldrich	C5138
Hyaluronidase	Sigma-Aldrich	H1136
Collagenase XI	Sigma-Aldrich	C7657
DMSO	Merck Millipore	317275
Cultrex Basement Membrane Extract	R&D Systems	3432-005-01
Polyethylenimine Linear	Polysciences	24765
DAPI	Roche	10236276001
GdCl ₃	Sigma-Aldrich	4399770
AG490	MCE	HY-12000
3-Deazaadenosine hydrochloride	MCE	HY-W013332A
N-Acetyl-L-cysteine	Sigma-Aldrich	A7250
S-(5'-Adenosyl)-L-methionine	Sigma-Aldrich	A7007
Recombinant Human TNF- α	R&D SYSTEMS	210-TA-010
Recombinant Human IL-1 β	R&D SYSTEMS	201-LB-005
Recombinant Human IFN- γ	R&D SYSTEMS	285-IF-100
Human CXCL10 ELISA Kit	Invitrogen	CHC2363
Human CCL2 ELISA Kit	Invitrogen	88-7399-88
Human SAM ELISA Kit	MEIMIAN	MM-13267H1
Human SAH ELISA Kit	MEIMIAN	MM-13268H1
Human GSH/GSSG ELISA Kit	Beyotime	S0053
Dichlorofluorescein diacetate	Sigma-Aldrich	2044-85-1
Metformin	MCE	HY-17471A
CCK-8	Abcam	ab228554
Apoptosis analysis kit	eBioscience	88-8005-72
EnVision System	Dako	K5007
Opal 7-Color Automation IHC Kit	Perkinelmer	NEL801001KT
TRIZOL Reagent	Life Technology	AM9738
5X All-In-One RT Master Mix	abm	G486
SYBR Green Real-Time PCR Master Mix	TOYOBO	QPS-201
IntraPrep Permeabilization Reagent	Beckman Coulter	A07803